

# Curie Temperature, Electrical and Magnetic Properties of In<sup>3+</sup> Substituted Yttrium Iron Garnet

R. G. Vidhate<sup>1</sup>, R.B. Kavade<sup>2</sup>, J. M. Bhandari<sup>3</sup>, K. M. Jadhav<sup>4</sup>

<sup>1</sup>Anandrao Dhonde Alias Babaji Mahavidyalaya, Kada, Beed.

<sup>2</sup>Bhagwan Mahavidyalaya, Ashti, Beed.

<sup>3</sup>Gandhi college Kada, Beed

<sup>4</sup>Department of physics MGM University, Aurangabad

## ABSTRACT

In<sup>3+</sup> was added in to yttrium iron garnet (YIG). Samples, with a nominal composition of Y<sub>3</sub>In<sub>x</sub>Fe<sub>5-x</sub>O<sub>12</sub> with x= 0.0, 0.2 and 0.4 were prepared by a solid-state sintering method. The samples were characterized by X-ray diffraction technique. The X-ray diffraction studies of compositions revealed the formation of single phase cubic structure with lattice constant ranging from 12.37 to 12.43 Å. The FTIR spectra of typical samples are taken in the range of 500-4000cm<sup>-1</sup>. IR spectra show typical absorption bands indicating the garnet nature of samples. The D.C. electrical resistivity  $\rho_{d.c.}$  Was measured in the temperature range 300-725 K. The results of a.c. susceptibility exhibit normal ferrimagnetic ordering which decreases with substitution of non-magnetic In<sup>3+</sup> ions in place of Fe<sup>3+</sup> ions. The effect of 'In<sup>3+</sup>' substitution in YIG shows that the saturation magnetization (Ms) decreases slowly for Y<sub>3</sub>Fe<sub>5</sub>O<sub>12</sub> (x = 0.0, 0.2 and 0.4).

**Keywords :** Yttrium iron garnet, indium, structural and electrical study.

## I. INTRODUCTION

Mixed metal oxides with iron (III) oxides as their main component are known as ferrites. Historically ferrites represent an important category of materials, which are in great demands due to their numerous applications in many fields. The electrical and magnetic properties of ferrites are strongly dependent on their chemical composition and their method of preparation [1, 2]. It is important to optimize the electrical and magnetic properties of ferrites, for desired applications. Due to their interesting properties scientists, researchers and engineers are still interested in designing the various types of ferrites material substituted with different cations with different valencies and prepared by different techniques.

In the various types of ferrites rare earth garnet especially yttrium iron garnet (YIG) is of great importance for scientist and technologist because of their applications in microwave communication devices such as circulators, oscillators, gyrators and phase shifters because of its small ferromagnetic resonance line-width, high electrical resistivity and low dielectric loss in microwave regions in many fields [3]. Yttrium iron garnet (YIG) is microwave ferrite, which in polycrystalline form has specific characteristics. The magnetic and

crystallographic properties of the magnetic iron garnet have been studied by many workers [4-7]. Substituted iron garnets have found extensive use in wide band non reciprocal microwave devices [8].

## II. EXPERIMENTAL

The samples of  $\text{In}^{3+}$  substituted  $\text{Y}_3\text{In}_x\text{Fe}_{5-x}\text{O}_{12}$  garnets with  $x = 0.0, 0.2$  and  $0.4$  were prepared by well-known double sintering ceramic method in which a molar ratio of analytical  $\text{Y}_2\text{O}_3$ ,  $\text{Fe}_2\text{O}_3$  and  $\text{In}_2\text{O}_3$  (all 99.99% pure AR grade chemicals, Mumbai) were mixed thoroughly in stoichiometric proportions and then ground to very fine powder by using agate mortar for about 3 hr. These mixtures in powder form were pre-sintered in a Indfur Programmable muffle furnace at  $1200^\circ\text{C}$  for 24 hr and cooled to room temperature slowly at the rate of  $2^\circ\text{C}/\text{min}$ . The samples were reground and re-fired at  $1350^\circ\text{C}$  for 30 hr and slowly cooled to room temperature at the rate of  $2^\circ\text{C}/\text{min}$ ., and then reground for 1 hr. The fine powdered sample was pelletized under the pressure 5 ton/inch<sup>2</sup>.

The electrical measurements were carried out by means of two probe method. The samples in the form of discs were polished well to have smooth parallel surfaces, and then these surfaces were coated with silver paste as a contact material for the electrical measurements. The temperature was measured by using chromel-alumel thermocouple in contact with the surface of the samples. The d.c. electrical resistivity  $\rho_{\text{d.c.}}$  was measured in the temperature range 300-725 K.

## III. RESULT AND DISCUSSION

Mixed garnet ferrites system under investigation has been structurally investigated by X-ray diffraction technique. The typical XRD pattern shows the reflections namely (321), (400), (420), (422), (431), (521), (611), (444), (640), (642), (800), (842). No extra peaks other than cubic structure have been observed in the XRD pattern. The Bragg peaks are sharp and intense. The lattice parameters are calculated using XRD data and are given in table-1. It is observed from table-1 that lattice constant increases with increase in indium content 'x'. The ionic radii of yttrium ( $0.89\text{\AA}$ )  $\text{Fe}^{3+}$  is ( $0.67\text{\AA}$ ) and indium ( $0.81\text{\AA}$ ) hence we observe variation in the lattice parameter with indium substitution. The bulk density of all samples was measured using Archimedes principle and values are tabulated in table-1. Bulk density increases with increase in indium content 'x'. Using the values of molecular weight and volume of the sample X-ray density was calculated. The values of X-ray density are also listed in Table-1. X-ray density increase with composition 'x'. The observed variation in X-ray density is attributed to increase in volume of the samples. The crystallographic parameters (lattice constant, X-ray density) are in good agreement with reported values [9]. The most intense peak (420) of XRD pattern was used to evaluate particle size of the samples. The particle size was calculated by using Scherer's formula, the values of particle size for all the composition is listed in Table-1.

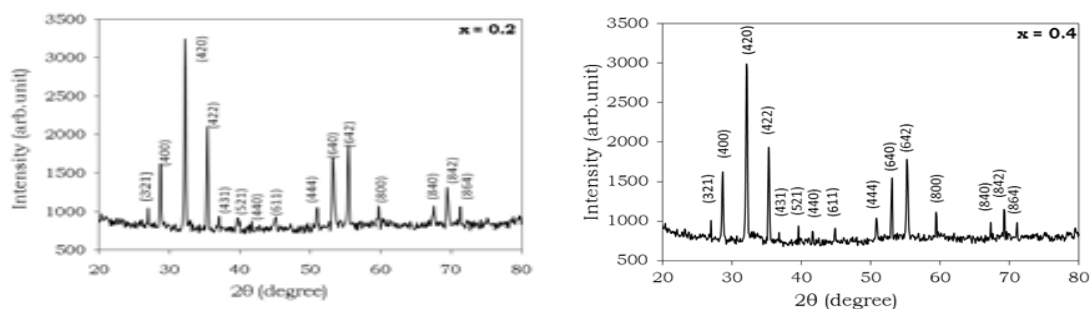


**Figure 1. Typical XRD patterns of  $\text{Y}_3\text{In}_x\text{Fe}_{5-x}\text{O}_{12}$  ( $x = 0.2$  and  $0.4$ )**

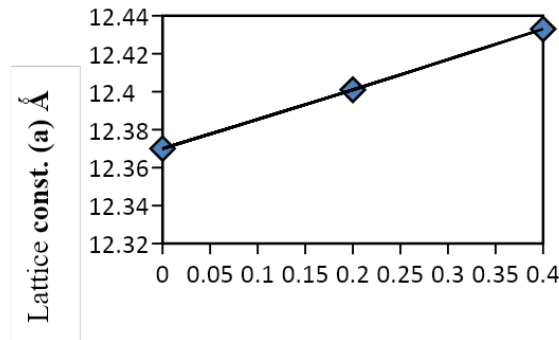


**Figure.2 Lattice constant 'a' versus Comp. 'x'**  
 $Y_3In_xFe_{5-x}O_{12}$  ( $x = 0.0, 0.2$  and  $0.4$ ).

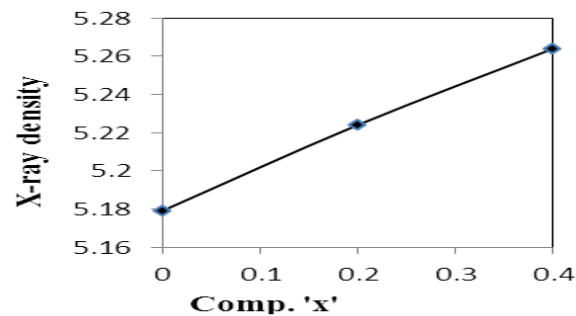


**Figure.3 Variation of X-ray density of 'dx' Versus composition 'x'**

**Table 1. Lattice constant (a), X-ray Density (dx), Bulk Density (db), Porosity (P) and Particle Size (t) of  $Y_3In_xFe_{5-x}O_{12}$ .**

x	a (Å)	dx (gm/cm <sup>3</sup> )	db (gm/cm <sup>3</sup> )	P (%)	t (μm)
0.0	12.370	5.179	4.13	20.25	3.42
0.2	12.401	5.224	4.19	19.97	3.25
0.4	12.433	5.264	4.26	19.07	3.17

IR spectra show typical absorption bands indicating the garnet nature of the samples. The band positions obtained from IR spectra are given in Table-3. The vibrational frequency depends upon the cation mass, cation oxygen bonding force, distance etc. From IR spectra, it is revealed that, a broad band appears at around 611 cm<sup>-1</sup>, 547 cm<sup>-1</sup> and 670 cm<sup>-1</sup>, assignable to the stretching mode of the tetrahedral in the YIG and this indicates that the crystallization of samples is more complete [10-12]. The values of absorption bands are given in Table 2. Our results on IR studies are in good agreement with the literature reports. [13]

**Table 2. Vibrational Band Frequencies ( $\nu_1, \nu_2, \nu_3, \nu_4$ ) of  $Y_3In_xFe_{5-x}O_{12}$ , for Samples  $x = 0.0$  and  $0.2$**

x	$\nu_1$ (cm <sup>-1</sup> )	$\nu_2$ (cm <sup>-1</sup> )	$\nu_3$ (cm <sup>-1</sup> )	$\nu_4$ (cm <sup>-1</sup> )
0.0	547.1	611.9	670.1	---
0.2	547.1	605.5	861.0	914.0

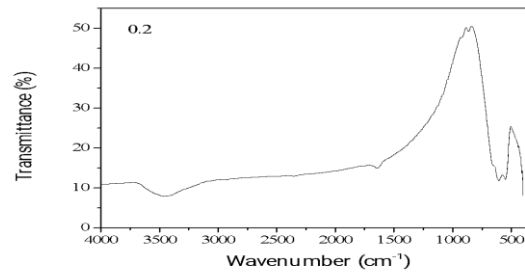
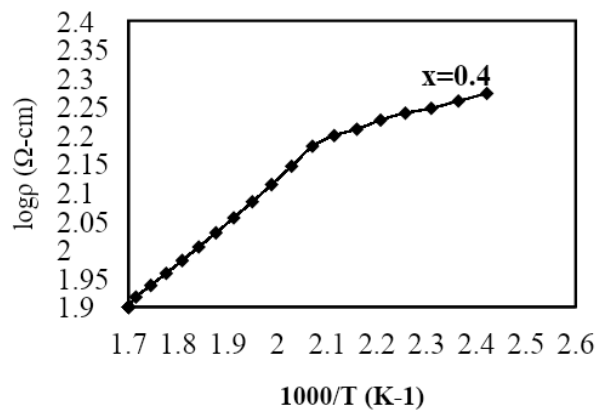


**Figure 4. Typical IR Spectra of  $Y_3In_xFe_{5-x}O_{12}$  of Typical Sample  $x = 0.2$**

#### IV. ANALYSIS OF ELECTRICAL RESISTIVITY

The D. C. electrical resistivity ( $\rho$ ) measurements for all the samples of  $Y_3In_xFe_{5-x}O_{12}$  garnet system were carried out in the temperature range of 300-725 K. Plots of  $\log \rho$  Vs  $1000/T$  are shown in Fig.6. It is observed from resistivity plots that, D.C. electrical resistivity decreases with increase in temperature. The plot exhibits a relatively sharp kink, which divides the curve in two parts. The resistivity plots obeys Arrhenius relation given by the equation,



$$\rho = \rho_0 e^{\frac{\Delta E_p}{kT}} e^{\frac{\Delta E_f}{kT}} \quad (1)$$

Using the above relation and from the resistivity plot, the activation energy for two regions that is ferrimagnetic and paramagnetic was calculated and the values are given in table 3. It is observed from table 3 that, activation energy decreases with increase in  $In^{3+}$  ions. The experimental results on D.C. electrical resistivity studies closely matches with those reported in the literature [17].

**Table 3. Activation Energy ( $\Delta E$ ) in Paramagnetic ( $E_p$ ) and Ferrimagnetic ( $E_f$ ) Region of  $Y_3In_xFe_{5-x}O_{12}$**

$x$	$E_p$ (eV)	$E_f$ (eV)	$\Delta E$ (eV)
0.0	0.25	0.13	0.12
0.2	0.19	0.10	0.09
0.4	0.13	0.06	0.07

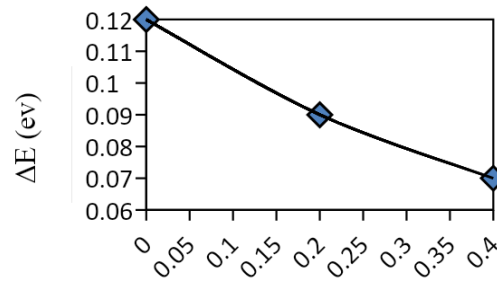


**Figure 4. Variation of Activation Energy ( $\Delta E$ ) Versus Composition  $x$  of  $Y_3In_xFe_{5-x}O_{12}$**

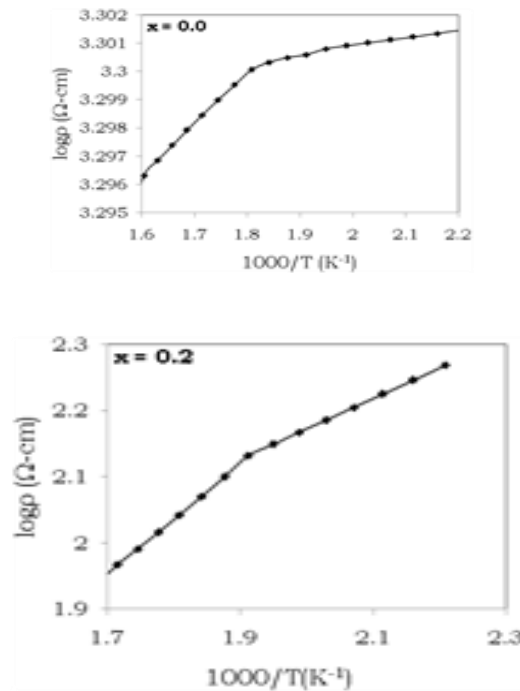


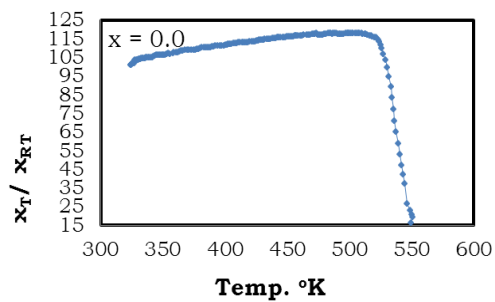
**Figure 5. Variation of  $\log \rho$  Versus  $1000/T$  of  $Y_3In_xFe_{5-x}O_{12}$  ( $x = 0.0, 0.2$  and  $0.4$ ).**

## V. ANALYSIS OF CURE TEMPERATURE MEASUREMENTS

The temperature dependence of relative a.c. susceptibility  $\chi_{(T)}/\chi_{(RT)}$  for all samples with  $x = 0.0, 0.2$  and  $0.4$  is shown in Fig.6. The results of a.c. susceptibility exhibit normal ferrimagnetic ordering which decreases with substitution of non-magnetic  $In^{3+}$  ions in place of  $Fe^{3+}$  ions. Using the susceptibility plots, the Curie temperature ( $T_C$ ) for all the samples was obtained and the values are listed in Table 4. It can be seen from table that the Curie temperature decreases with increasing  $x$  [18] as shown in Fig 6. The decrease in Curie temperature is related to the replacement of magnetic  $Fe^{3+}$  ions by non-magnetic  $In^{3+}$  ions. Thus, the magnetic properties of  $Y_3Fe_5O_{12}$  are influenced by the substitution of  $In^{3+}$  ions.

**Table 4. Curie Temperature ( $T_c$ ) Data Measured from Loria Technique, A.C. Susceptibility Technique and D. C. Resistivity of  $Y_3In_xFe_{5-x}O_{12}$ .**

$x$	$T_c$ (K)		
	Loria Technique	A. C. susceptibility	D. C. Resistivity
0.0	550	550	550
0.2	525	504	526
0.4	477	468	483



$x$	$M_s$ (emu/gm)	$M_r$ (emu/gm)	$H_c$ (Oe)	( $M_r/M_s$ )
0.0	31.1800	0.4100	14.05	0.0130
0.2	27.0400	1.6100	14.91	0.0610
0.4	24.9678	0.1485	20.05	0.0059

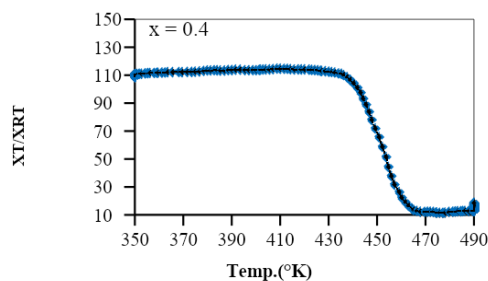
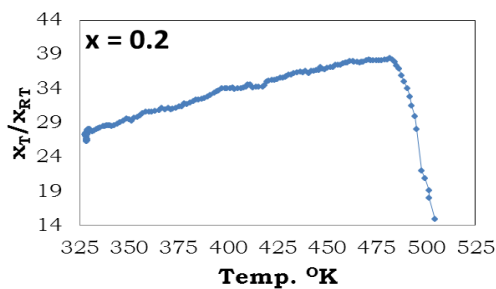
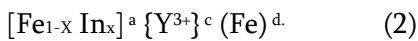


**Figure 6. Variation of A. C. Susceptibility ( $\chi_T/\chi_{RT}$ ) with Temperature (T) of  $Y_3In_xFe_{5-x}O_{12}$ . ( $x=0.0, 0.2$  and  $0.4$ )**

## VI. Analysis of Magnetization

The saturation magnetization ' $M_s$ ' and the Magneton number ' $n_B$ ' (the saturation magnetization per formula unit in Bohr Magneton) at 300 K obtained from the hysteresis loop technique for  $x = 0.0, 0.2$  and  $0.4$  are summarized in Table 5. Fig 7 shows variation of Magneton number ' $n_B$ ' with  $\text{In}^{3+}$  content  $x$ . From field dependence of magnetization and observed magnetic moments (Table 5), it is clear that, samples with  $x = 0.0, 0.2$  and  $0.4$  shows ferrimagnetic behavior which decreases with  $\text{In}^{3+}$  content  $x$ . It can be seen from Fig 7 that, the spontaneous magnetization decreases very slowly with  $x$ . In the present series  $\text{Y}_3\text{In}_x\text{Fe}_{5-x}\text{O}_{12}$ ,  $\text{In}^{3+}$  is substituted for  $\text{Fe}^{3+}$  ions. Based on Neel's theory of ferrimagnetism in ferrites, [19] the substitution of non-magnetic ions like  $\text{In}^{3+}$  in place of  $\text{Fe}^{3+}$  ions at octahedral [a] can lead to a decrease in saturation magnetization as shown in Table 5 and Fig.7. However, the observed magneton number decreases with non-magnetic  $\text{In}^{3+}$  ions. Assuming that  $\text{In}^{3+}$  ions occupy octahedral [a] sites,  $\text{Y}^{3+}$  ions occupy dodecahedral {c} sites and  $\text{Fe}^{3+}$  ions [a] and (d) sites, the cation distribution can be written as



Using above proposed cation distribution, the magneton number for each sample was calculated. The calculated values of magneton number are listed in Table 5 it is observed from Table 5 that calculated magneton number and observed do not match with each other. The observed discrepancy in the magneton number can be explained on the basis of Yafet Kittle angle [20].

Using hysteresis plot (Fig 7), coercivity and remanence magnetization are obtained and the values are presented in Table 5. The low values of coercivity represents that, the particle size of the prepared samples is in micron range.

**Table 5. Saturation Magnetization ( $M_s$ ), Remanence Magnetization ( $M_r$ ), Coercivity ( $H_c$ ) and Remanence Ratio ( $M_r/M_s$ ) of  $\text{Y}_3\text{In}_x\text{Fe}_{5-x}\text{O}_{12}$ .**

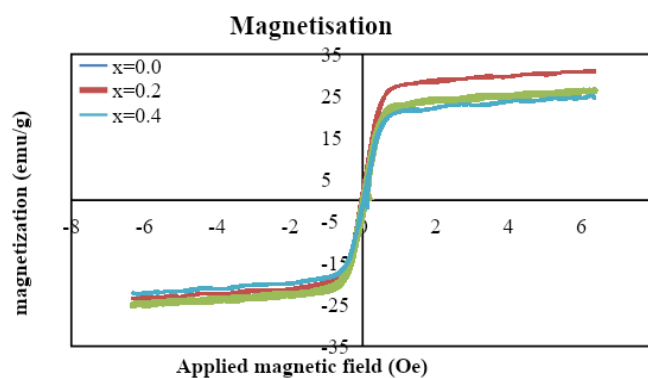


**Figure 7. Variation of Magneton Number ' $n_B$ ' with  $\text{In}^{3+}$  Content  $x$ .**

## VII. CONCLUSION

The garnet system In-YIG was prepared by a solid-state sintering method. The parameter lattice constant increases slightly with  $\text{In}^{3+}$  substitution. IR spectra show typical absorption bands indicating the garnet nature

of the samples. It is observed from resistivity plots that, D.C. electrical resistivity decreases with increase in temperature and activation energy decreases with increase in  $\text{In}^{3+}$  ions. The Curie temperature ( $T_c$ ) obtained from a. c. susceptibility data decreases very slowly with increasing  $x$ . The effect of ' $\text{In}^{3+}$ ' substitution in YIG shows that the saturation magnetization ( $M_s$ ) decreases slowly for  $\text{Y}_3\text{Fe}_5\text{O}_{12}$  ( $x = 0.0, 0.2$  and  $0.4$ ). The magnetic data can be explained assuming collinear spin ordering model.

## VIII. REFERENCES

- [1] H. B. Sharma, H N K Sharma and Chandra Prakash. Ibetombi Soibam, Sumitra phanjoubam, Ind. J. Phys. 83 (3) (2009) 285.
- [2] B. K. Kuanr, P. K. Singh, P. Kisan, N. Kumar, S.L.N. Rao, G.P. Srivastava. J. Appl. Phys. 8 (1986) 63
- [3] Guo Cuijing, Zhang Wei, Ji Rongjin, Zeng Yanwei, J. Magn. Mater. 323 (2011) 611.
- [4] S. Geller and M. A. Gilleo, J. Phys. chem. Solids 3 (1957) 30.
- [5] M. A. Gilleo and Geller S., Phys. Rev. 110, (1958) 73.
- [6] M. A. Gilleo, J. Phys. Chem. Solids 13 (1960) 33.
- [7] E. E. Anderson, J. Phys. Soc. Japan Suppl. 17 (1962) 365.
- [8] B. Lax and K. Button, Microwave ferrites and ferri-magnetics", McGraw-Hill Book Co. Inc New York (1962).
- [9] J. Richard Cunningham and Elmer E. Anderson, J. Appl. Phys. 32, (1961) S388.
- [10] A. M. Hotmeister, K. R. Campbell, J. Appl. Phys. 72 (1992) 638.
- [11] M. Ristic, I. Nowik, S. Popovic, I. Felner, S. Music, J. Mater. Lett. 57 (2003) 2584.
- [12] Zhongjun Cheng, Hua Yang, Lianxiang Yu, Yuming Cui, Shouhua Feng, J. Magn. Mater. 302 (2006) 259.
- [13] A. Kenneth, Wickersheim, J. Appl. Phys. 32 (1961) 205S.
- [14] J. Smit and H. P. J. Wijn, Ferrites, New York, Wiley, 1959.
- [15] Hongjie Zhao Ji Zhou Yang Bai Zhilun Gui Longtu Li J. Magn. Mater. 280 (2004) 208.
- [16] K. Iwachi, Jap. Appl. Phys. 10 (1971) 1520.
- [17] I. D. Lomako, V.I. Pavlov, and N.Ya. Shishkin, Crystallo. Reports, 48 (2003) 116.
- [18] S. Geller, Williams, H. J. G. P. Espinosa, R. C. Sherwood Phys. Rev. 136 (1964) A1650.
- [19] J. S. Smart, Am. J. Phys. 23 (1955) 356.
- [20] Y. Yafet and C. Kittel, Phys. Rev. 87 (1952) 290.